

gfpop: an R Package for Univariate Graph-Constrained Change-point Detection

Vincent Runge
Université d'Évry*

Toby Dylan Hocking
Northern Arizona University

Gaetano Romano
Lancaster University

Fatemeh Afghah
Northern Arizona University

Paul Fearnhead
Lancaster University

Guillem Rigail
INRAE - Université d'Évry

Abstract

In a world with data that change rapidly and abruptly, it is important to detect those changes accurately. In this paper we describe an R package implementing an algorithm recently proposed by [Hocking et al. \[2017\]](#) for penalised maximum likelihood inference of constrained multiple change-point models. This algorithm can be used to pinpoint the precise locations of abrupt changes in large data sequences. There are many application domains for such models, such as medicine, neuroscience or genomics. Often, practitioners have prior knowledge about the changes they are looking for. For example in genomic data, biologists sometimes expect peaks: up changes followed by down changes. Taking advantage of such prior information can substantially improve the accuracy with which we can detect and estimate changes. [Hocking et al. \[2017\]](#) described a graph framework to encode many examples of such prior information and a generic algorithm to infer the optimal model parameters, but implemented the algorithm for just a single scenario. We present the **gfpop** package that implements the algorithm in a generic manner in R/C++. **gfpop** works for a user-defined graph that can encode the prior information of the types of change and implements several loss functions (Gauss, Poisson, Binomial, Biweight and Huber). We then illustrate the use of **gfpop** on isotonic simulations and several applications in biology. For a number of graphs the algorithm runs in a matter of seconds or minutes for 10^5 datapoints.

Keywords: change-point detection, constrained inference, maximum likelihood inference, dynamic programming, robust losses.

1 Introduction

1.1 Standard multiple change-point model

Multiple change-point models are designed to find abrupt changes in a signal. In the standard Gaussian noise model, we have data $Y_{1:n} = (Y_1, \dots, Y_n)$ where each data point, Y_t , is an independent random variable with $Y_t \sim \mathcal{N}(\mu_t, \sigma^2)$ and $t \mapsto \mu_t$ is piecewise constant. The goal is to estimate the number and position of the changes, that is to find all t such that $\mu_t \neq \mu_{t+1}$ from the observed data $(y_t)_{t=1, \dots, n}$. A classical way to proceed is to optimize the log-likelihood

*E-mail: vincent.runge@univ-evry.fr

by fixing the number of changes. It is also possible to penalize each change by a positive penalty β and minimize in $\mu = (\mu_1, \dots, \mu_n)^T \in \mathbb{R}^n$ the following least squares criterion:

$$Q_n^{std}(\mu) = \sum_{t=1}^n (y_t - \mu_t)^2 + \beta \sum_{t=1}^{n-1} I_{\mu_t \neq \mu_{t+1}} ,$$

where $I \in \{0, 1\}$ is the indicator function. In both cases, fast dynamic programming algorithms can solve the related optimisation problem exactly [Killick et al., 2012, Rigaiil, 2015, Maidstone et al., 2017].

1.2 Constrained multiple change-point model

In many applications, it is desirable to constrain the parameters of successive segments [Hocking et al., 2015a, Maidstone et al., 2017, Jewell et al., 2018, Baranowski and Fryzlewicz, 2014]. This means that the μ parameter is restricted by inequalities to a subset of \mathbb{R}^n . Arguably, the simplest and most studied case is isotonic regression [Barlow et al., 1972]. In this case the goal is to minimize in μ the constrained least-squares criterion:

$$Q_n^{iso}(\mu) = \sum_{t=1}^n (y_t - \mu_t)^2 , \text{ subject to the constraint } \mu_t \leq \mu_{t+1}, \forall t \in \{1, \dots, n-1\}.$$

The obtained estimator is piecewise constant, which makes the link with the multiple change-point problem.

More generally, we may want to impose more complex patterns, such as unimodality [Stout, 2008] or a succession of up and down changes [Hocking et al., 2015a] to detect peaks. There are very efficient algorithms for the isotonic and unimodal cases [Best and Chakravarti, 1990, Stout, 2008] at least if the number of changes is not penalised. For more complex constraints like the up-down pattern, Hocking et al. [2017] proposed an exact algorithm. This algorithm is a generalization of the functional dynamic programming algorithm of Rigaiil [2015] and Maidstone et al. [2017]. The algorithm allows one to penalize or constrain the number of changes. The algorithm also allows one to consider robust losses, including the biweight loss, instead of the least-squares criterion for assessing fit to the data. In the case of non-constrained (standard) multiple change-point detection the biweight loss has good statistical properties [Fearnhead and Rigaiil, 2018]. The simulations of Bach [2018] in the context of isotonic regression also show the benefit of such losses.

1.3 Contribution

Hocking et al. [2017] described a graph-framework to encode many prior constraints on how parameters change at each changepoint, and a generic algorithm to infer the optimal model parameters. However, they implemented the algorithm in a single scenario: where the mean alternately increases then decreases and a Poisson loss. The `gfpop` package implements their algorithm in a generic manner in R/C++, and works for a user-defined graph and implements several loss functions.

The constraints in `gfpop` are modelled by a graph. The graph can be viewed as a representation of the transition kernel of a specific continuous-state Hidden Markov Model (HMM). At each time t the signal can be in a number of states. These states are the nodes of the graph. Possible transitions between states at time t and $t+1$ are represented by the edges of the graph. Each edge is associated to 3 elements: a constraint (e.g. $\mu_t \leq \mu_{t+1}$), a penalty (possibly null) and a loss function (cost associated to a data-point).

1.4 Outline

In Section 2 we formally define the graphs and explain their connection to HMM. We also provide numerous graph examples to illustrate the versatility of our framework. In Section 3 we present the optimization problem solved by our package. In Section 4 we go through the main functions of the package. We illustrate in Section 5 the use of our package on various real datasets. Finally, using simulations we compare in Section 6 the result of our package with those of standard isotonic packages and show the benefit of using robust losses and penalising the number of segments.

2 Constraint graphs and change-points model as a HMM

We begin by recasting the standard and constrained multiple change-point problem as a continuous HMM with a particular transition kernel represented as a graph. In `gfpop` the set of transitions is constant over time leading to a collapsed representation of the graph. We then formalize the concept of a valid signal or path, that is satisfying all constraints. We eventually present a number of examples.

2.1 Transition kernel and graph of constraints

Standard multiple change-point model as a HMM. It is possible to recast the classic multiple change-point model as a Hidden Markov Model with a continuous state space. Precisely, we define random variables Z_1, \dots, Z_n in \mathbb{R} or some interval $[a, b]$. We consider a transition kernel $k(x, y) \propto I_{x=y} + e^{-\beta} I_{x \neq y}$. Finally, in the Gaussian case, observations are obtained as $(Y_i | Z_i = \mu) \sim \mathcal{N}(\mu, \sigma^2)$. The Bayesian Network of this model is given in Figure 1.

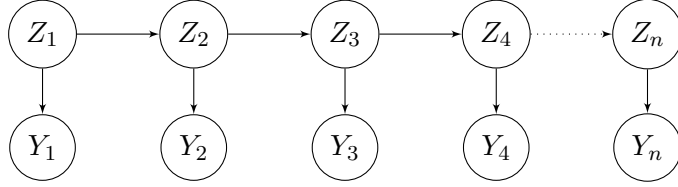


Figure 1: Multiple change-point model as a Hidden Markov Model.

Here the state space is in \mathbb{R} . The `gfpop` algorithm of [Hocking et al. \[2017\]](#) allows one to consider a more complex state space in $\mathcal{S} \times \mathbb{R}$ where \mathcal{S} is a finite set. In that case the transition kernel is more complex and can be described using a graph. Below, we first present the graph and then explain how it is linked to the transition kernel.

Graph of constraints. The graph of constraints \mathcal{G}_n is an acyclic directed graph defined as follows.

1. Nodes are indexed by time $t \in \{1, \dots, n\}$ and a state $s \in \mathcal{S} = \{1, \dots, S\}$;
2. We include two undefined states $\#, \emptyset$ for the starting nodes, $v_0 = (0, \#)$, and arrival nodes, $v_{n+1} = (n+1, \emptyset)$;
3. Edges are transitions between consecutive “time” nodes of type $v = (t, s)$ and $v' = (t+1, s')$. Edges e are then described by a triplet $e = (t, s, s')$ for $t \in \{0, \dots, n\}$;
4. Each edge $e = (t, s, s')$ is associated with

- an indicator function $\mathcal{I}_e : \mathbb{R} \times \mathbb{R} \rightarrow \{0, 1\}$ constraining successive means¹ μ_t and μ_{t+1} . For example an edge e with the corresponding indicator function $\mathcal{I}_e(\mu_t, \mu_{t+1}) = I_{\mu_t \leq \mu_{t+1}}$ ensures that means are non-decreasing (the usual indicator $I_x = 1$ if x is true, and is zero otherwise);
- a penalty $\beta_e \geq 0$ which is used to regularize the model (larger penalty values result in more costly change-points and thus fewer change-points in the optimal model);
- a loss function γ_e for datapoint y_{t+1} ².

Transition kernel. Coming back to our HMM representation of change-point models, the transition from state (s, μ_t) to (s', μ_{t+1}) (up to proportionality) is

- $k((s, \mu_t), (s', \mu_{t+1})) = \exp(-\beta_e) \mathcal{I}_e(\mu_t, \mu_{t+1})$, if there is an edge $e = (t, s, s')$ in the graph;
- $k((s, \mu_t), (s', \mu_{t+1})) = 0$ if there is no edge $e = (t, s, s')$ in the graph.

Some simple examples. In Figures 2 and 3 we provide the corresponding graphs for the standard and isotonic models. Notice that the only difference is that the transitions between nodes $(t, 1)$ and $(t + 1, 1)$ are restricted to non-decreasing means in the isotonic case.

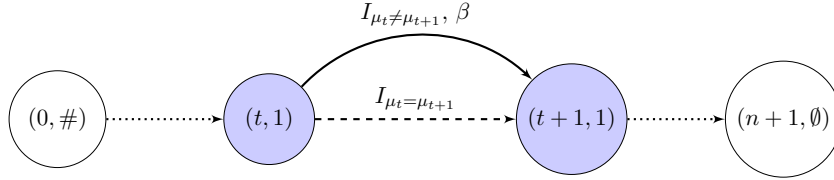


Figure 2: Graph of constraints for the standard multiple change-point model. We have $\mathcal{S} = \{1\}$, the loss function is always the ℓ_2 (Gaussian loss). The penalty is omitted when equal to zero.

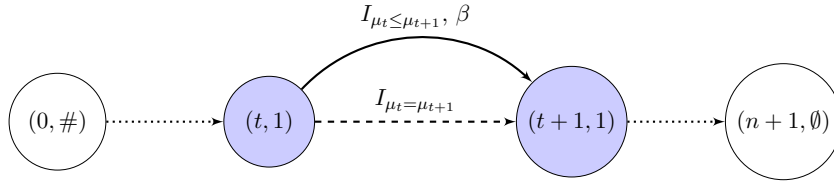


Figure 3: Graph of constraints for the isotonic change-point model. We have $\mathcal{S} = \{1\}$, the loss function is always the ℓ_2 . The penalty is omitted when equal to zero.

2.2 Collapsed graph of constraints

In **gfpop** we only consider transitions that do not depend on time. We then collapse the previous graph structure. To be specific, we have a single node for each s and a transition from node s to s' if there is a transition from (t, s) to $(t + 1, s')$ in the full graph structure. In Figures 4 and 5 we provide the corresponding collapsed graphs for the standard and isotonic models.

¹We call this parameter a mean for convenience but some models consider changes in variance or in other natural parameters.

²The loss function can be edge-specific: see Figure 24 and the graph construction in Subsection 4.1.

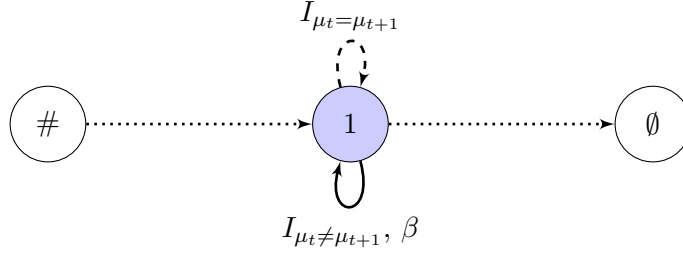


Figure 4: Collapsed graph of constraints for the standard multiple change-point model. We have $\mathcal{S} = \{1\}$. The loss function is always the ℓ_2 . The penalty is omitted when equal to zero.

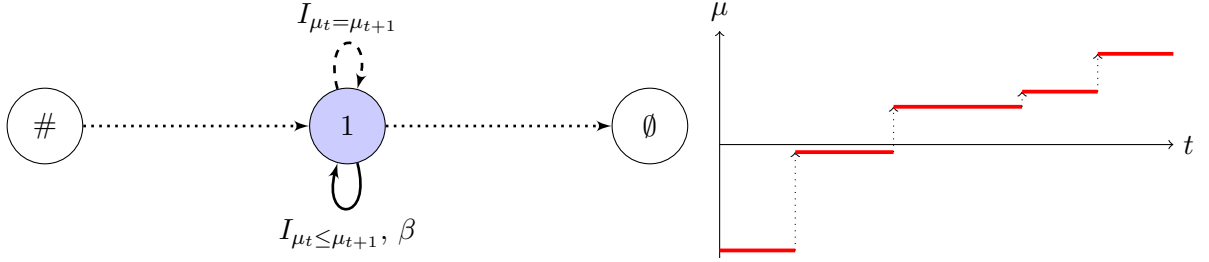


Figure 5: (Left) Collapsed graph of constraints for the isotonic change-point model. We have $\mathcal{S} = \{1\}$, the loss function is always the ℓ_2 . The penalty is omitted when equal to zero. (Right) In red, a piecewise constant function validating the graph of constraints.

Path and constraints validation. In Section 3 we discuss maximum likelihood inference for such models. To define this maximum properly we formalize the notion of a signal validating our constraints through the concept of a valid path in the collapsed graph.

A path p of the collapsed graph \mathcal{G}_n is a collection of $n+2$ nodes (v_0, \dots, v_{n+1}) with $v_0 = (0, \#)$, $v_{n+1} = (n+1, \emptyset)$ and $v_t = (t, s_t)$ for $t \in \{1, \dots, n\}$ and $s_t \in \{1, \dots, S\}$. In addition, the path is made of $n+1$ edges named e_0, \dots, e_n . Recall that each edge e_t is associated to a penalty β_{e_t} , a loss γ_{e_t} and a constraint \mathcal{I}_{e_t} . A vector $\mu \in \mathbb{R}^n$ validates the path p if for all $t \in \{1, \dots, n-1\}$, we have $\mathcal{I}_{e_t}(\mu_t, \mu_{t+1}) = 1$ (true). We write $p(\mu)$ to say that the vector μ checks the path p .

The starting and arrival edges e_0 and e_n are exceptions. For them there are neither indicator function nor associated penalty (see Figures 2 and 3). However, there is a loss function γ_{e_0} for the starting edge to add the first data-point.

Definition. From now on when we use the word “graph” we mean the collapsed graph of constraints. In this graph, the triplet notation (t, s, s') for edges is replaced by (s, s') . We remove the time dependency also for edges associated with starting and arrival nodes to simplify notations (even if in that case, there is a time dependency).

2.3 A few examples

We present a few constraint models and their graphs. Some models have been already proposed in the literature, but not necessarily using our HMM formalism.

- (Up - Down) To model peaks [Hocking et al. \[2015b\]](#) proposed an up-down constraint using two states $\mathcal{S} = \{Up, Dw\}$. Transitions from Dw to Up are forced to go up $I_{\mu_t \leq \mu_{t+1}}$.

Transitions from Up to Dw are forced to go down $I_{\mu_t \geq \mu_{t+1}}$. The graph of this model is given in Figure 6.

- (Up - Exponentially Down) To model pulses Jewell et al. [2018] proposed a model where the mean decreases exponentially between positive spikes. In that case a unique state with two transitions is sufficient. The first transition corresponds to an up change $I_{\mu_t \leq \mu_{t+1}}$ and the second to an exponential decay $I_{\alpha \mu_t = \mu_{t+1}}$ with $0 < \alpha < 1$. The graph of this model is given in Figure 7.
- (Segment Neighborhood) One often considers a known number segment D [Auger and Lawrence, 1989]. This is encoded by a graph with D states, $\mathcal{S} = \{1, \dots, D\}$. From any $d \in \mathcal{S}$ there are two transitions to consider. One from d to d with constraint $I_{\mu_t = \mu_{t+1}}$ and one from d to $d + 1$ with constraints $I_{\mu_t \neq \mu_{t+1}}$. The graph of this model for $D = 3$ is given in Figure 8.
- (At least 2 data-points per segment) It is often desirable to get sufficiently long segments. For at least 2 data-points one should consider two states $\mathcal{S} = \{Wait, Seg\}$. There are 3 transitions to consider one from Seg to $Wait$ with the constraint $I_{\mu_t \neq \mu_{t+1}}$, one from Seg to Seg with $I_{\mu_t = \mu_{t+1}}$ and one from $Wait$ to Seg with $I_{\mu_t = \mu_{t+1}}$. The graph of this model is given in Figure 9. This can be extended to p data-points. The graph for at least 3 data-points per segment is given in Appendix A (Figure 18).

In Appendix A we provide a few more examples. In particular, we reformulate the collective anomaly model of Fisch et al. [2018] as a constrained model.

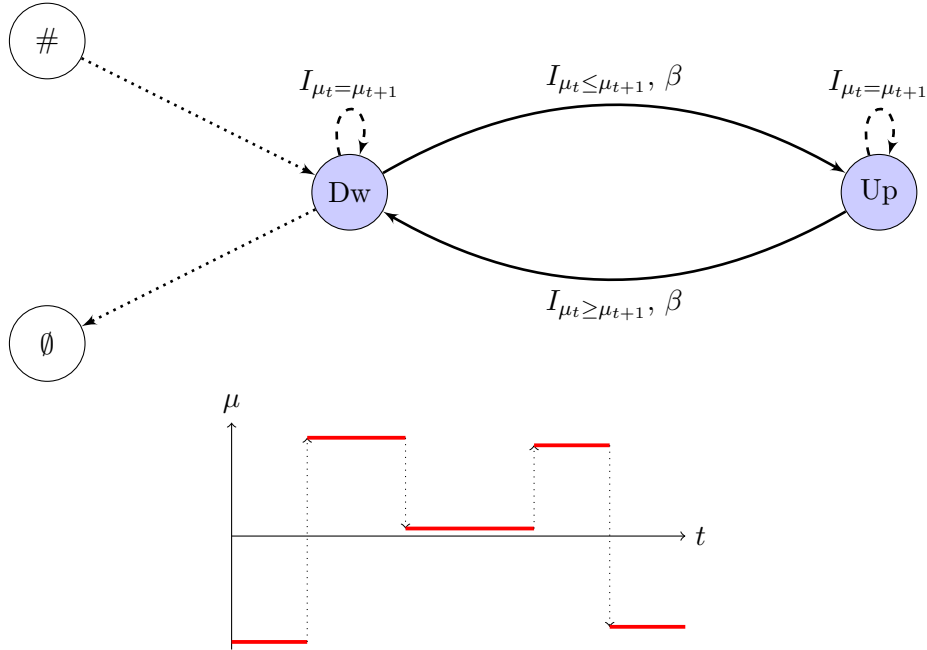


Figure 6: (Top) Graph for the up-down change-point model proposed in Hocking et al. [2015b]. We have $\mathcal{S} = \{Up, Dw\}$, the loss function is always the ℓ_2 . The penalty is omitted when equal to zero. (Bottom) In red, a piecewise constant function validating the graph of constraints. The penalty is omitted when equal to zero.

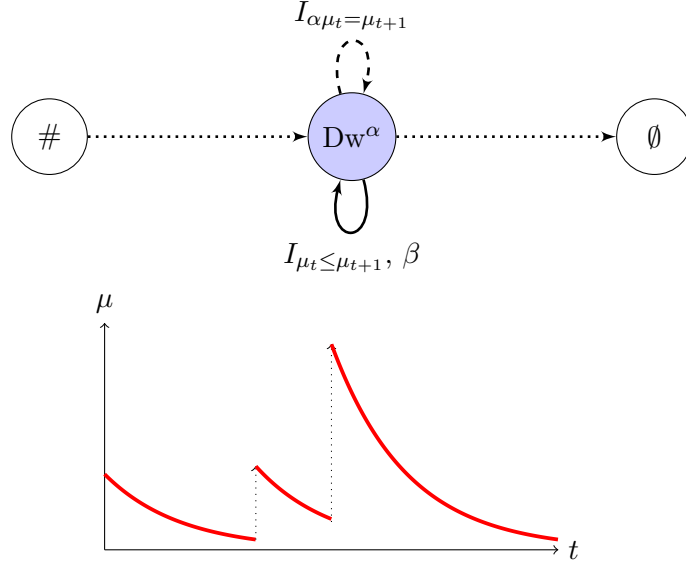


Figure 7: (Top) Graph for the up - exponential decrease change-point model proposed in [Jewell et al. \[2018\]](#). We have $\mathcal{S} = \{Dw^\alpha\}$, the loss function is always the ℓ_2 . The penalty is omitted when equal to zero. (Bottom) In red, a function validating the graph of constraints.

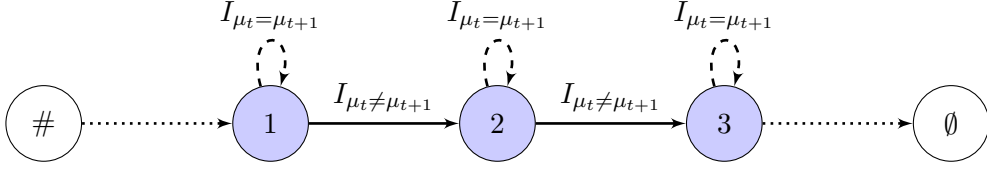


Figure 8: Graph for the 3-segment change-point model. We have $\mathcal{S} = \{1, 2, 3\}$, the loss function is always the ℓ_2 . The penalty is always equal to zero.

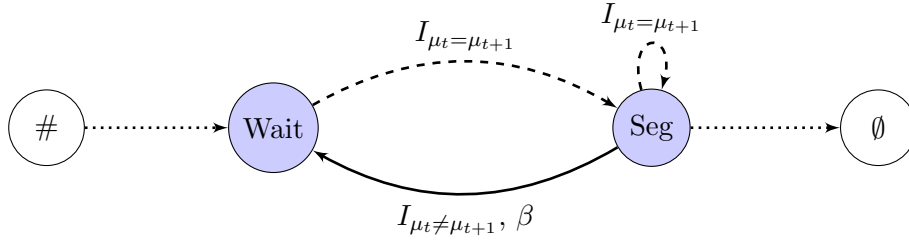


Figure 9: Graph for the at least 2 data-points per segment change-point model. We have $\mathcal{S} = \{Wait, Seg\}$, the loss function is always the ℓ_2 . The penalty is omitted when equal to zero.

3 Optimization problem solved by gfpop

3.1 Penalised maximum likelihood

We now present the constrained change-point optimization problem. The goal is to minimize the negative log-likelihood over all model parameters that validate the constraints (see Subsection 2.2):

$$Q_n = \min_{\substack{p=(v,e) \in \mathcal{G}_n \\ \mu | p(\mu)}} \left\{ \sum_{t=1}^n (\gamma_{e_t}(y_t, \mu_t) + \beta_{e_t}) \right\}.$$

It is a discrete optimisation problem. A naive exploration of the 2^{n-1} change-point positions is not feasible in practice. Due to the constraints, segments are dependent and Q_n cannot be written as a sum over all segments. Therefore the algorithms of Auger and Lawrence [1989], Jackson et al. [2005], Killick et al. [2012] are not applicable.

Hocking et al. [2017] have shown that it is possible to optimize Q_n using functional dynamic programming techniques. The idea is to consider the quantity Q_n as a function of the mean and the state of the last data-point:

$$Q_n^s(\theta) = \min_{\substack{p=(v,e) \in \mathcal{G}_n \\ \mu | p(\mu) \\ \mu_n=\theta, v_n=(n,s)}} \left\{ \sum_{t=1}^n (\gamma_{e_t}(y_t, \mu_t) + \beta_{e_t}) \right\}, \quad (1)$$

where we use the subscript n to denote the number of data points analysed, s to denote the state of the most recent transition, and θ the mean of the last data point.

By construction each Q_n^s is a piecewise function and can be defined as the pointwise minimum of a finite number of functions, with the form of these functions depending on the loss used. In the package three analytical decompositions for the pieces of Q_n^s are implemented:

L2 decomposition. $f_1 : \theta \mapsto 1$, $f_2 : \theta \mapsto \theta$ and $f_3 : \theta \mapsto \theta^2$. This decomposition allows one to consider Gaussian (least-square), biweight and Huber loss functions;

Lin-log decomposition. $f_1 : \theta \mapsto 1$, $f_2 : \theta \mapsto \theta$ and $f_3 : \theta \mapsto \log(\theta)$. This decomposition allows one to consider loss functions for Poisson and exponential models. It is also possible to consider a change in the variance of a Gaussian distribution of mean 0³;

Log-log decomposition. $f_1 : \theta \mapsto 1$, $f_2 : \theta \mapsto \log(\theta)$ and $f_3 : \theta \mapsto \log(1 - \theta)$. This decomposition allows one to consider loss functions for the binomial and negative binomial likelihoods.

As in the Viterbi algorithm for finite state space HMM, it is possible to define an update formula linking the set of functions $\{\theta \mapsto Q_{n-1}^s(\theta), s \in \mathcal{S}\}$ to $\theta \mapsto Q_n^{s'}(\theta)$ for all states s' . Computationally, the update is applied per interval using some edge-dependent operators described in the following subsection [Rigaill, 2015, Maidstone et al., 2017, Hocking et al., 2017].

3.2 Operators and update-rule for gfpop

Let us consider a transition from s to s' at step n . Its edge is (s, s') and its associated constraint is $I_{(s,s')}$. The gfpop algorithm involves calculating the best (θ, s) to reach state (θ', s') , i.e

³To be clear, in that case the log-likelihood is $\frac{1}{2} \log(\frac{1}{\sigma^2}) - \frac{y_t^2}{2\sigma^2}$ and we get the Lin-Log decomposition by taking $\theta = \frac{1}{\sigma^2}$

minimising the functional cost while satisfying the constraint $I_{(s,s')}$. Formally this is defined as an operator:

$$O_n^{s,s'}(\theta') = \min_{\theta|I_{(s,s')}(\theta,\theta')} \{Q_n^s(\theta)\}.$$

Operator calculation For a general constraint I and a general function Q_n^s it is not easy to compute $O_n^{s,s'}$. Recall that $Q_n^s(\theta)$ are piecewise analytical, i.e. they can be exactly represented by a finite set of real-valued coefficients. For algorithmic simplicity [Hocking et al. \[2017\]](#) requires that $O_n^{s,s'}(\theta)$ has the same analytical decomposition per interval (L2, Lin-Log or Log-Log).

In practise here are the constraints we can accommodate.

L2 decomposition: any linear constraint, e.g $a\mu_t + b\mu_{t+1} + c \leq 0$ or $a\mu_t + b\mu_{t+1} + c = 0$;

Lin-log decomposition: any proportional constraint e.g $a\mu_t \leq \mu_{t+1}$ or $a\mu_t = \mu_{t+1}$;

Log-log decomposition: only the two inequalities $\mu_t \leq \mu_{t+1}$ or $\mu_t \geq \mu_{t+1}$.

Note that constraints can be combined by considering more than one edge from one state to another. In particular, for L2 decomposition the constraint $|\mu_{t+1} - \mu_t| \geq c$ can be implemented using $\mu_t + c \leq \mu_{t+1}$ or $\mu_t \geq \mu_{t+1} + c$. This constraint encodes the idea of detecting sufficiently large changes (also called relevant changes) described in [Dette and Wied \[2016\]](#).

Computationally, it is possible to compute $O_n^{s,s'}(\theta)$ by scanning from left to right or from right to left all intervals which correspond to a different functional form of $Q_n^s(\theta)$ (See examples in [Hocking et al. \[2017\]](#)).

Update-rule. Given this operator function we can now define the update rule used by the gfpop algorithm.

$$Q_{n+1}^{s'}(\theta) = \min_{s|\exists \text{ edge}(s,s')} \left\{ O_n^{s,s'}(\theta) + \gamma_{(s,s')}(y_{n+1}, \theta) + \beta_{(s,s')} \right\}. \quad (2)$$

For simplicity, we do not describe the update for initial and final steps. The proof of this update rule is very similar to the proof of the Viterbi algorithm and is given in [Appendix B](#). It follows the strategy of [Hocking et al. \[2017\]](#). Notice also that recovering the optimal set of change-points from all Q_1^s, \dots, Q_n^s by backtracking is not straightforward. We provide some details in [Appendix C](#).

3.3 How to choose the loss function and penalty ?

The choice of the loss function γ is linked to the choice of the noise model. This choice is not necessarily easy. For example for continuous data it might make sense to consider the least square error [[Picard et al., 2005](#)]; in the presence of outliers considering a robust loss is natural [[Fearnhead and Rigall, 2018](#)]; and for discrete data a Poisson loss is often used [[Hocking et al., 2017](#)]. It is our experience that visualizing the data beforehand is a good way to avoid simple modeling mistakes.

The choice of the penalty β is critical to select the number of change-points. In the absence of constraint several penalties have been proposed. A penalty of $\beta = 2\sigma^2 \log(n)$ was proposed by [Yao and Au \[1989\]](#). It tends to work well when the number of changes is small. More complex penalties exist, e.g [Zhang and Siegmund \[2007\]](#), [Lebarbier \[2005\]](#), [Baraud et al. \[2009\]](#). For penalties that are concave in the number of segments one can run the gfpop algorithm for

various values of β and recover several segmentations (with a varying number of change-points) [Killick et al., 2012]. This can be done efficiently using the CROPS algorithm [Haynes et al., 2014]. In labeled data sets, supervised learning algorithms can be used to infer an accurate model for predicting penalty values β [Rigaill et al., 2013].

For models with constraints, to the best of our knowledge there is very little statistical literature available. The paper of Gao et al. [2017] describes a penalty in the isotonic case but it was not calibrated. It is our experience that the penalties proposed for the unconstrained case tend to work reasonably well, although they are probably sub-optimal from a statistical perspective.

4 The gfpop package

4.1 Graph construction

Our **gfpop** package deals with collapsed graphs for which all the cost functions γ have the same decomposition (L2, Lin-log or Log-log). All other characteristics are local and fixed per edge. The graph \mathcal{G}_n (see Subsection 2.2) is defined in the **gfpop** package by a collection of edges.

Edge parameters. An edge is a list of four main elements:

- `state1` : the starting node defined by a string;
- `state2` : the arrival node defined by a string;
- `type` : a string equal to “null”, “std”, “up”, “down” or “abs” defining the type of constraints between successive nodes respectively corresponding to indicators $I_{\mu_t=\mu_{t+1}}$, $I_{\mu_t \neq \mu_{t+1}}$, $I_{\mu_t+c \leq \mu_{t+1}}$, $I_{\mu_t \geq \mu_{t+1}+c}$ and $I_{|\mu_{t+1}-\mu_t| \geq c}$;
- `penalty` : the penalty β_e associated to this edge (it can be zero);

and some optional elements:

- `decay` : a number between 0 and 1 for the mean exponential decay (in case type is “null”) corresponding to the constraint $I_{\mu_{t+1}=\alpha\mu_t}$;
- `gap` : the gap c between successive means of the “up”, “down” and “abs” types;
- `K` : the threshold for the Biweight and Huber losses ($K > 0$);
- `a` : the slope for the Huber robust loss ($a \geq 0$).

An example of edge. We can define an edge `e1` with the function `Edge` as:

```
e1 <- Edge(state1 = "Dw", state2 = "Up", type = "up", penalty = 10, gap = 0.5)
```

which is an edge from node `Dw` to node `Up` with an up constraint, penalty $\beta = 10$ and a minimal jump size of 0.5.

An example of graph. We provide an example of graph for collective anomalies detection with the `gfpop` package given in Figure 24 (see Fisch et al. [2018]):

```
> graph(
+   Edge(state1 = "mu0",state2 = "mu0", penalty = 0, K = 3),
+   Edge(state1 = "mu0",state2 = "Coll", penalty = 10, type = "std"),
+   Edge(state1 = "Coll",state2 = "Coll", penalty = 0),
+   Edge(state1 = "Coll",state2 = "mu0", penalty = 0, type = "std", K = 3),
+   StartEnd(start = "mu0", end = c("mu0", "Coll")),
+   Node(state = "mu0", min = 0, max = 0)
+ )
```

	state1	state2	type	parameter	penalty	K	a	min	max
1	mu0	mu0	null	1	0	3	Inf	NA	NA
2	mu0	Coll	std	0	10	Inf	Inf	NA	NA
3	Coll	Coll	null	1	0	Inf	Inf	NA	NA
4	Coll	mu0	std	0	0	3	Inf	NA	NA
5	mu0	<NA>	start	NA	NA	NA	NA	NA	NA
6	mu0	<NA>	end	NA	NA	NA	NA	NA	NA
7	Coll	<NA>	end	NA	NA	NA	NA	NA	NA
8	mu0	mu0	node	NA	NA	NA	NA	0	0

Notice that the graph is encoded into a data-frame.

Note 1. Most graphs (as the previous one) contain recursive edges, that is edges with the same starting and arrival node. The absence of this edge forces a change and is useful to enforce a minimal segment length (see Figures 9 and 18).

Note 2. In the `gfpop` graph definition, a starting (resp. arrival) node is a state s for which there exists an edge between the starting $v_0 = (0, \#)$ (resp. arrival $v_{n+1} = (n+1, \emptyset)$) node and s (See Subsection 2.2). These specific states are defined using function `StartEnd`. If not specified, all nodes are starting and arrival nodes. The range of values for parameter inference at each node can be constrained using function `Node`.

Some default graphs. We included in function `graph` the possibility to directly build some standard graphs. Here is an example for the isotonic case corresponding to Figure 5:

```
> graph(type = "isotonic", penalty = 12)
```

	state1	state2	type	parameter	penalty	K	a	min	max
1	Iso	Iso	null	1	0	Inf	Inf	NA	NA
2	Iso	Iso	up	0	12	Inf	Inf	NA	NA

Three other standard graph types are: “std”, “updown” corresponding to Figures 4 and 6 and “relevant” corresponding to Figure 19.

4.2 The `gfpop` function

The `gfpop` function takes as an input the data and the graph and runs the algorithm. It returns a set of change-points and the non-penalised cost (that is the value of the fit to the data ignoring the penalties for adding changes). It also returns the mean value and the state of each segment. The boolean “forced” value indicates whether a linear inequality constraint is active, which means that the μ_t and μ_{t+1} values lie on the frontier defined by the inequality constraint. Below we illustrate the use of the `gfpop` function for various graphs and loss functions.

Gaussian model with an up-down graph. Here is an example with a Gaussian cost and a standard penalty of $2\log(n)$ for the up-down graph.

```
> n <- 1000
> myData <- dataGenerator(n, c(0.1,0.3,0.5,0.8,1), c(1,2,1,3,1), sigma = 1)
> myGraph <- graph(penalty = 2*log(n), type = "updown")
> gfpop(data = myData, mygraph = myGraph, type = "mean")

$changepoints
[1] 98 293 500 800 1000
$states
[1] "Dw" "Up" "Dw" "Up" "Dw"
$forced
[1] 0 0 0 0
$parameters
[1] 1.0661402 1.9773539 0.9498154 2.9469084 1.1014419
$globalCost
[1] 1059.566
```

The response contains four vectors. A vector `changepoints` contains the last index of each segment, a vector `states` gives the nodes in which lie the successive parameter values of the `parameters` vector. The vector `forced` is a vector of booleans of size 'number of segments - 1' with a 1 when the transition between two states (nodes) has been forced. The `globalCost` is the non-penalised cost.

Gaussian Robust biweight model with an up-down graph. Below we illustrate the use of the biweight loss on data where 10% of the data points are outliers. We use the biweight loss with $K = 3$ and an "updown" graph with a difference of at least 1 between consecutive means.

```
> n <- 1000
> chgtpt <- c(0.1,0.3,0.5,0.8,1)
> mydata <- dataGenerator(n, chgtpt, c(0,1,0,1,0), sigma = 1)
> mydata <- mydata + 5*(rbinom(n, 1, 0.05)) - 5*(rbinom(n, 1, 0.05))
> beta <- 2*log(n)
> myGraph <- graph(
+   Edge("Dw", "Up", type = "up", penalty = beta, gap = 1, K = 3),
+   Edge("Up", "Dw", type = "down", penalty = beta, gap = 1, K = 3),
+   Edge("Dw", "Dw", type = "null", K = 3),
+   Edge("Up", "Up", type = "null", K = 3),
+   StartEnd(start = "Dw", end = "Dw"))
> gfpop(data = mydata, mygraph = myGraph, type = "mean")

$changepoints
[1] 98 300 500 799 1000
$states
[1] "Dw" "Up" "Dw" "Up" "Dw"
$forced
[1] 0 0 1 0
$parameters
[1] -0.15963245 1.05776459 -0.04670309 0.95329691 -0.10528826
$globalCost
[1] 1057.899
```

Poisson model with isotonic up graph. We provide an example with a Lin-log cost decomposition with Poisson data constrained to increasing up changes with a doubling constraint on successive means.

```

> n <- 1000
> chgtpt <- c(0.1,0.3,0.5,0.8,1)
> mydata <- dataGenerator(n, chgtpt, c(1,3,5,7,12), sigma = 1, type = "poisson")
> beta <- 2*log(n)
> myGraph <- graph(type = "isotonic", gap = 2)
> gfpop(data = mydata, mygraph = myGraph, type = "poisson")

$changepts
[1] 3 100 299 799 1000
$states
[1] "Iso" "Iso" "Iso" "Iso" "Iso"
$forced
[1] 1 0 0 1
$parameters
[1] 0.5177665 1.0355330 2.8844221 6.1563193 12.3126386
$globalCost
[1] -6171.899

```

Negative binomial model with 3-segment graph. The parameters to find are probabilities and we restrict the inference to 3 segments. The optional parameter “all.null.edges” in graph function automatically generates “null” edges for all nodes.

```

> mygraph <- graph(
+   Edge("1", "2", type = "std", penalty = 0),
+   Edge("2", "3", type = "std", penalty = 0),
+   StartEnd(start = "1", end = "3"),
+   all.null.edges = TRUE)
> data <- dataGenerator(n = 1000, changepts = c(0.3,0.7,1),
+   parameters = c(0.2,0.25,0.3), type = "negbin", sigma = 1)
> gfpop(data, mygraph, type = "negbin")

$changepts
[1] 300 689 1000
$states
[1] "1" "2" "3"
$forced
[1] 0 0
$parameters
[1] 0.2126783 0.2697592 0.3266846
$globalCost
[1] 2172.154

```

4.3 Some additional useful functions in gfpop

Data generator. As demonstrated in the previous examples, the dataGenerator function can be used to simulate n data-points using a distribution of type “mean”, “poisson”, “exp”, “variance” or “negbin”. Standard deviation parameter σ and decay γ are specific to the Gaussian mean model, whereas size is linked to the R “rnbino” function from R stats package.

Standard deviation estimation. For many real-data-sets examples, we are obliged to estimate the standard deviation from the observed data. This value is then used to normalize the data or to be included in edge penalties. The sdDiff returns such an estimation with the default HALL method [Hall et al., 1990] well suited for time series with change-points.

A plotting function. We defined a plotting function `plot`, which shows data-points and the results of the `gfpop` function on a unique graph. The user has to explicitly use the `data` parameter as in following example.

```
data <- dataGenerator(1000, c(0.4,0.8,1), c(1,2,1), "mean", sigma = 3)
g <- gfpop(data,
  graph(type = "std", penalty = 2*sdDiff(data)^2*(log(1000))),
  type = "mean")
plot(x = g, data = data)
```

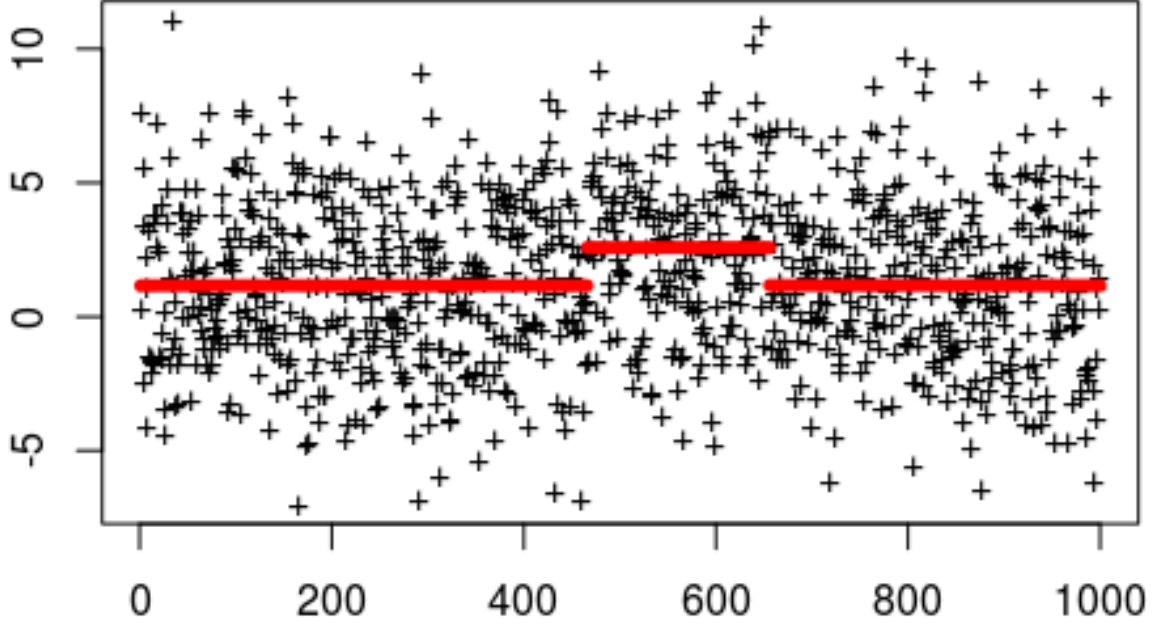


Figure 10: The red piecewise constant signal is the μ vector find by the `gfpop` function. It is built using response vectors changepoints and parameters.

5 Modeling real data with graph-constrained changepoint models

In this section we illustrate the use of our package on several real datasets. For each application we illustrate several possible sets of constraints and briefly discuss their benefit.

5.1 Gaussian model for DNA copy number data

We consider DNA copy number data, which are biological measurements that characterize the number of chromosomes in cell samples. Abrupt changes along chromosomes in these data are important indicators of severity in cancers such as neuroblastoma [Schleiermacher et al., 2010]. The non-constrained Gaussian segmentation model has been shown to have state-of-the-art change-point detection accuracy in these data [Hocking et al., 2013].

However, in some high-density copy number data sets, this model incorrectly detects small changes in mean which are not relevant [Hocking and Rigaiil, 2012]. One such data set is shown in Figure 11, which also has positive and negative labels from an expert genomic scientist that indicated regions with (1breakpoint) or without (0breakpoints) relevant change-points.

We used these labels to quantify the accuracy of three unconstrained Gaussian change-point models with several different penalties β .

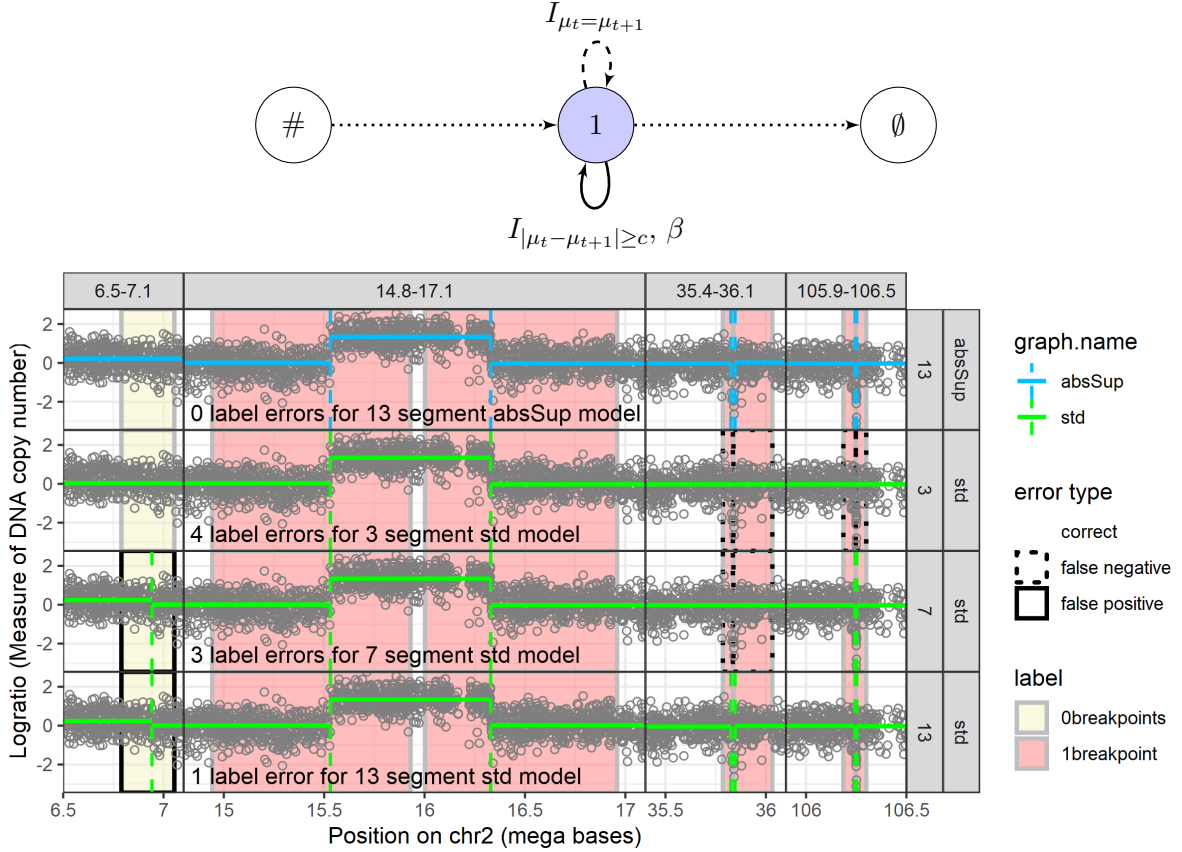


Figure 11: **Top graph:** Relevant change-point model; all changes are forced to be greater than a in absolute value. **Below:** Four subsets/windows of a DNA copy number profile (panels from left to right) and four change-point models (panels from top to bottom). **Top panel with blue model:** abs model with 13 segments enforces the constraint that the absolute value of each change must be at least 1, $|\mu_{t+1} - \mu_t| \geq 1$, which achieves zero label errors in these data. **Bottom panels with green models:** each model with no constraints between adjacent segment means has label errors (4 false positives for 3 segments, 2 false positives and 1 false negative for 7 segments, 1 false positive for 13 segments).

- The model with 13 segments predicts a change-point in each positive label (0/6 false negatives), but predicts one change-point in the negative label (1 false positive), for a total of 1 incorrectly predicted label. (bottom panel)
- The model with 7 segments predicts a change-point in four positive labels (2/6 false negatives), and also predicts the false positive change-point in the negative label, for a total of 3 incorrectly predicted labels. (second panel from bottom)
- The model with 3 segments predicts a change-point in only two positive labels (4/6 false negatives), and predicts no change-point in the negative label (0/1 false positive), for a total of 4 incorrectly predicted labels. (second panel from top)

We computed all non-constrained Gaussian models from 1 to 20 segments for these data, and none of them were able to provide change-point predictions that perfectly match the

expert-provided labels (each model had at least one false positive or false negative). It is thus problematic to use the unconstrained changepoint model in this context, because none of the unconstrained models achieve zero label errors.

To solve this problem we propose a graph (Figure 11, top graph) which enforces only “relevant” change-points $|\mu_{t+1} - \mu_t| \geq c$, for some relevant threshold $c > 0$. For the DNA copy number data set, we set $c = 1$ and choose β such that the algorithm returns 13 segments (Figure 11, top panel with blue model). The proposed model predicts a change-point in each of the positive labels, but does not predict a change-point in the negative label. The proposed graph-constrained change-point model is therefore able to predict change-points that perfectly match the expert-provided labels.

5.2 Gaussian multi-modal regression for neuro spike train data

A changepoint model with exponential decreasing segments has been proposed for calcium imaging data from neuroscience [Jewell et al., 2018]. We fit this model to one calcium imaging data set (Figure 12, Right top) and observed that it is difficult to find a parameter that detects both labeled spikes (red rectangles). Part of the difficulty is the fact that there are two parameters to tune, the penalty β and also the exponential decay parameter γ .

We therefore propose a new multi-modal regression model (Isotonic up - Isotonic down graph shown in Figure 12, left) with only one parameter, the penalty β which controls the number of changes. In this model there are several modes, and the number of modes is controlled by the penalty β . Each mode consists of any number of up changes followed by any number of down changes. We observed that it is easy to find a penalty β which detects both labeled spikes. Overall these results indicate that the proposed multi-modal regression model (Isotonic up - Isotonic down) is promising for spike detection in calcium imaging data.

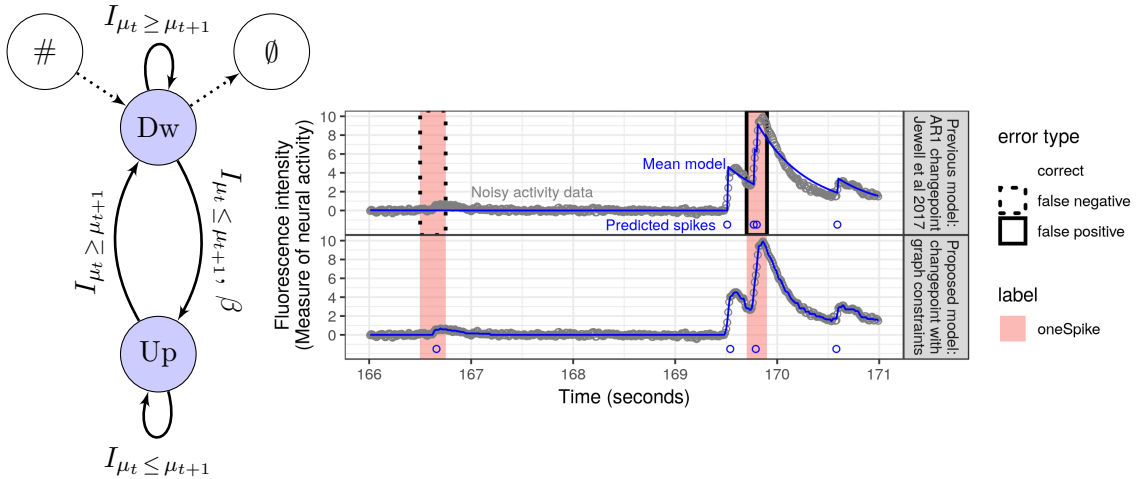


Figure 12: **Left:** Graph for multi-modal regression. **Right top:** In these data the previously proposed AR1 model misses a spike in the left label (false negative) and predicts two spikes where there should be only one in the right label (false positive). **Right bottom:** The proposed multi-modal regression model correctly detects one spike in each of the two labeled regions.

5.3 Gaussian nine-state model for electrocardiogram data

In the context of monitoring hospital patients with heart problems, electrocardiogram (ECG) analysis is one of the most common non-invasive techniques for diagnosing several heart ar-

rhythmia [Afghah et al., 2015]. A preliminary and fundamental step in ECG analysis is the detection of the QRS complex that leads to detecting the heartbeat and classifying the rhythms Mousavi and Afghah [2019]. Here, we utilize the proposed change-point detection method to locate the QRS complex in ECG waveforms. The ECG signals used in this study are extracted from the publicly available Physionet Challenge 2015 database PhysioNet [2015], Clifford et al. [2016] that includes measurements for three physiological signals (including ECG) for 750 patients. The resolution and frequency of each signal are 12bit and 250 Hz, respectively. Also, each signal has been filtered by a finite impulse response (FIR) band pass [0.05 to 40Hz] and mains notch filters.

Pan-Tompkins algorithm is one of the most common segmentation methods used for ECG analysis [Pan and Tompkins, 1985, Agostinelli et al., 2017]. This method uses a patient-specific threshold-based approach for real-time detection of the QRS complex in ECG signals, which represents the ventricular depolarization. In this algorithm, after a pre-processing step by a band-pass filter, the signal is passed through differentiation and squaring blocks to determine and amplify the slope of QRS, followed by a moving window integration step with an adaptive set of thresholds to determine the peaks. The detection thresholds are learned at the beginning of the algorithm and are calibrated periodically to follow the variations of the ECG signal.

Figure 14 (top) shows four seconds of ECG data for which we predicted the QRS complex using the well-known Pan-Tompkins method. The peak of each heartbeat should be predicted as R, but the algorithm incorrectly predicts S in two cases. In contrast the peak is correctly classified as R (bottom) using our proposed model with nine states (see Figure 13).

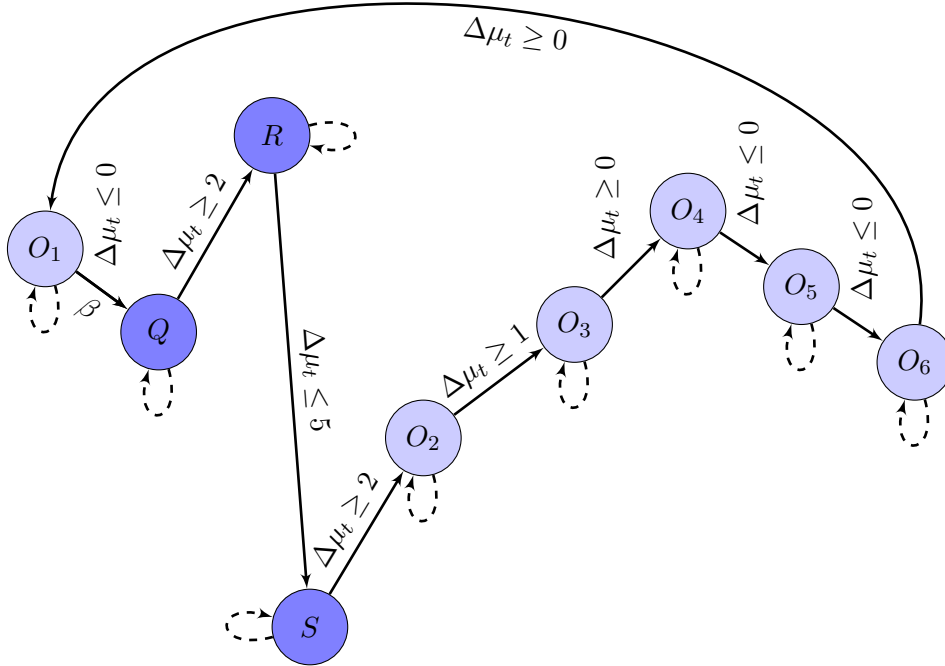


Figure 13: Graph structure of proposed nine-state constrained change-point model. The graph is cyclic: the last node O_1 is the first node O_1 . Only one transition (from O_1 to Q) to enter the QRS complex is penalised by a positive penalty $\beta = 8 \times 10^3$. We used the notation $\Delta\mu_t = \mu_{t+1} - \mu_t$. Transitions from state Q to state O_3 are constrained with a minimal gap size of 2, 5, 2 and 1. Due to lack of space, we removed the indicator function I on this graph. Dashed arrows correspond to $I_{\mu_t = \mu_{t+1}}$ transitions. The vertical position of the states gives information on the direction of the constrained changes.

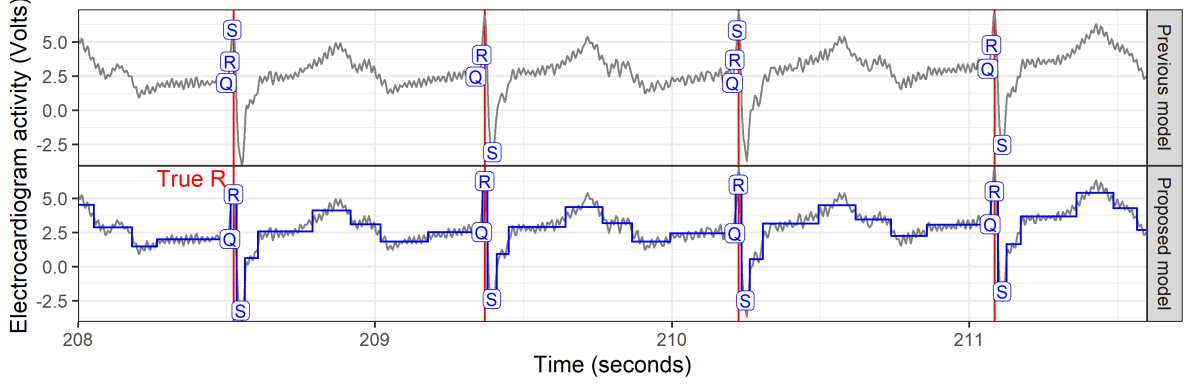


Figure 14: In these electrocardiogram data, it is important for models (blue) to accurately detect the QRS complex (Q is before the peak, R is the peak marked in red, S is the local minimum after the peak, other states o1–o6). **Top:** Previous model of Pan and Tompkins [1985] mistakenly predicts S at the peak. **Bottom:** proposed constrained change-point model accurately predicts R at each peak.

6 Utility of penalised isotonic regression models

Our package can be used with robust loss functions which have been shown to be useful in the presence of outliers [Fearnhead and Rigall, 2018] and in particular in the context of isotonic regression [Bach, 2018]. Here we illustrate this on simulations inspired by those of Bach [2018] (see Figure 15 with corrupted data). We compare our package using the isotonic model described in Figure 5 with several implementations of the PAVA algorithm [Best and Chakravarti, 1990, Mair et al., 2009].

Relative to the very fast $O(n)$ PAVA, our dynamic programming algorithm is slower. However, PAVA only works for the square loss and the non-penalised model (maximum number of changes). In contrast, **gfpop** can handle non-convex losses (such as the biweight loss) and can include a positive penalty in order to reduce the number of changes.

6.1 Parametrisation

gfpop. In all simulations we used **gfpop** with the graph of Figure 5 and a quadratic (l2) or a biweight loss (bw). We considered two different values for the penalty β : 0 and $2\sigma^2 \log(n)$, with σ^2 the true variance. Thus, we have 4 different algorithms of the **gfpop** function: **gfpop1** ($\beta = 0$, $K = 0$), **gfpop2** ($\beta = 2\sigma^2 \log(n)$, $K = 0$), **gfpop3** ($\beta = 0$, $K = 3\sigma$) and **gfpop4** ($\beta = 2\sigma^2 \log(n)$, $K = 3\sigma$).

Competitors. We compared the output of **gfpop** with those of 2 isotonic regression package functions:

- **isoreg** function of the **stats** package which is based on the very fast Pool adjacent violators algorithm for the ℓ_2 loss [Best and Chakravarti, 1990];
- **reg_1d** function developed in package **UnilsoRegression** which solves the isotonic regression problem for the ℓ_2 and ℓ_1 losses [Stout, 2008].

We also include a simple linear regression approach (**lm** function of the **stats** package) as a reference. In total we have 4 competitors (**lm**, **isoreg**, **reg_1d** with the ℓ_2 and ℓ_1 losses).

6.2 Simulated data

We focused on two types of increasing signals:

linear: as in Bach [2018] we consider linearly increasing time series with a signal

$$s_i = \alpha(i - \frac{n}{2}) \quad i = 1, \dots, n;$$

step-wise: as our package is devoted to change-point inference we also consider a step-wise increasing series (with 10 steps) with a signal

$$s_i = \lfloor \frac{10(i-1)}{n} \rfloor - \frac{n}{2}, \quad i = 1, \dots, n.$$

We consider three ways to corrupt the data.

Gaussian noise: here we simply add a Gaussian noise, with a variance σ^2 to the signal (i.e : $Y_i = s_i + \varepsilon_i$).

Student noise: we also considered a Student noise with a degree of freedom equal to 3.

Corrupted noise: in the most difficult scenario, suggested by Bach [2018], we randomly select a proportion p of data-points and multiply them by -1 and then add a Gaussian noise, i.e $Y_i = X_i s_i + \varepsilon_i$, where $X_i \sim \mathcal{B}(p)$ is a Bernoulli trial with probability p to get -1 and probability $1 - p$ to get 1 . We fix $p = 0.3$ for all simulations.

In total we have 6 scenarios (2 signals and 3 ways to corrupt the data). In Figure 15 we illustrate those 6 scenarios with $n = 10^4$ and $\sigma = 10$, which is an example of time series used in following simulations.

Criteria. To assess the quality of the results, we compute the Mean-Squared Error (MSE) as well as the ability to recover the true number of changes when there are changes in the data in the step-wise scenario.

6.3 A simple illustration

We begin by a simple illustration on a step-wise increasing signal with corrupted data. In Figure 16, we represent the data and the results of various approaches. We see that using a biweight loss our package in blue is closer to the true signal in black than other approaches.

In next Subsections we considered Monte-Carlo simulations to confirm this result: see Subsection 6.4 for the linear increasing scenario and Subsection 6.5 for the step-wise increasing scenario. The R code of these simulations can be found on the Github page https://github.com/vrunge/gfpop_Rsimu.

6.4 Linear signal

We simulate 100 linearly increasing time series and compute the mean of the MSE for each noise structure. The results are in Table 1. We highlight in bold the two best results in each row and also give the standard deviation (SD).

In the Gaussian case the ℓ_2 isotonic regression and **gfpop1** (with $\beta = 0$ and $K = \infty$) are better. For the Student and for the Corrupted scenarios the robust biweight loss with $\beta = 0$ is performing better in terms of MSE. Note that it is however much slower than PAVA. Including a penalty for change-points ($\beta_0 = 2\sigma^2 \log(n)$) deteriorates the results. This make sense as there are in fact no change-points in the data.

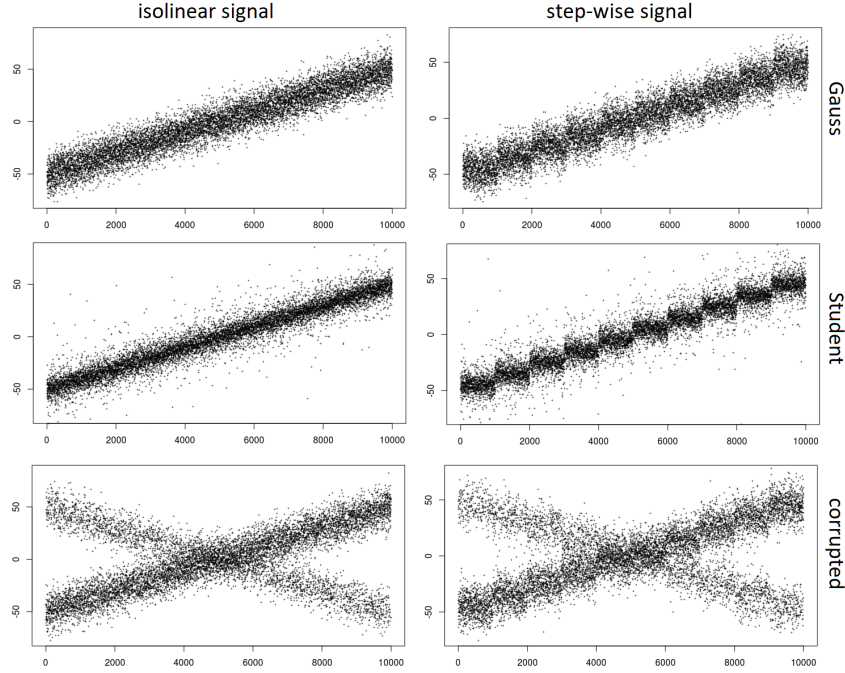


Figure 15: For the two types of signal, we show simulated data with $n = 10^4$ data-points and $\sigma = 10$ for the three different noises (Gauss, Student, corrupted).

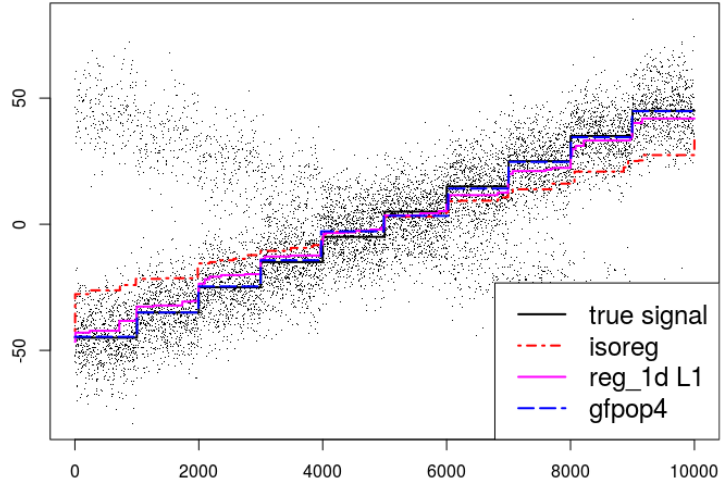


Figure 16: Isotonic regression with 30% of corrupted data in step-wise scenario with 10 steps. We have 10^4 data-points and $\sigma = 10$. **gfpop4** is close to the signal and with a number of segments equal to 10.

6.5 Iso-step signal

We simulate 100 step-wise increasing time series with 10 segments and compute the mean of the MSE for each noise structure. The results are in Table 2. We highlight in bold the two best results in each row and also give the standard deviation (SD).

In Gaussian and Student cases the penalised algorithms **gfpop3** and **gfpop4** with $\beta = \beta_0 = 2\sigma^2 \log(n)$ are better. For the corrupted scenario, we need the robust loss of algorithms **gfpop2** and **gfpop4** to get a much better MSE than other approaches. To confirm the benefit of using

Isolinear simulations	linear fit	isoreg ℓ_2	reg_1d ℓ_1	reg_1d ℓ_2	gfpop1 $\beta = 0$ ℓ_2	gfpop2 $\beta = 0$ $K = 3\sigma$	gfpop3 $\beta = \beta_0$ ℓ_2	gfpop4 $\beta = \beta_0$ $K = 3\sigma$
Gauss MSE (SD)	0.0190 (0.020)	0.714 (0.098)	0.712 (0.098)	1.08 (0.17)	0.826 (0.15)	0.931 (0.13)	2.60 (0.27)	3.10 (0.30)
Student MSE (SD)	0.0185 (0.19)	0.683 (0.12)	0.681 (0.12)	0.550 (0.077)	0.780 (0.17)	0.555 (0.076)	2.56 (0.24)	2.57 (0.22)
Corrupted MSE (SD)	299 (9.1)	298 (8.8)	298 (8.8)	28.7 (2.2)	294 (11)	4.05 (0.63)	301 (8.9)	7.23 (0.89)

Table 1: Mean squared errors $\text{MSE} = \frac{1}{n} \sum_{i=1}^n (\hat{s}_i - s_i)^2$ for different algorithms on linear simulations with its empirical standard deviation (SD). We consider three types of noise : Gaussian, Student and corrupted.

a penalised approach in Student case, we plot the distribution of the MSE for the five best algorithms in Figure 17.

Iso-step simulations	linear fit	isoreg ℓ_2	reg_1d ℓ_1	reg_1d ℓ_2	gfpop1 $\beta = 0$ ℓ_2	gfpop2 $\beta = 0$ $K = 3\sigma$	gfpop3 $\beta = \beta_0$ ℓ_2	gfpop4 $\beta = \beta_0$ $K = 3\sigma$
Gauss MSE (SD)	8.27 (0.022)	0.635 (0.11)	0.632 (0.10)	1.34 (0.30)	1.21 (0.78)	0.842 (0.16)	0.358 (0.12)	0.470 (0.17)
Student MSE (SD)	8.27 (0.024)	0.571 (0.15)	0.569 (0.15)	0.564 (0.14)	1.09 (1.0)	0.439 (0.13)	0.301 (0.15)	0.201 (0.073)
Corrupted MSE (SD)	304 (7.6)	300 (7.3)	300 (7.2)	30.1 (3.5)	297 (11)	3.57 (0.53)	301 (7.3)	3.17 (0.59)

Table 2: Mean squared errors $\text{MSE} = \frac{1}{n} \sum_{i=1}^n (\hat{s}_i - s_i)^2$ for different algorithms on step-wise simulations with its empirical standard deviation (SD). We consider three types of noise : Gaussian, Student and corrupted.

We also compare the ability of the different methods to estimate the number of steps. The average number of steps over 100 simulations is reported in Table 3. Only the penalised algorithms are able to recover the true number of steps (10). The choice of a good penalty in isotonic simulations is an area of ongoing research in statistics [Gao et al., 2017].

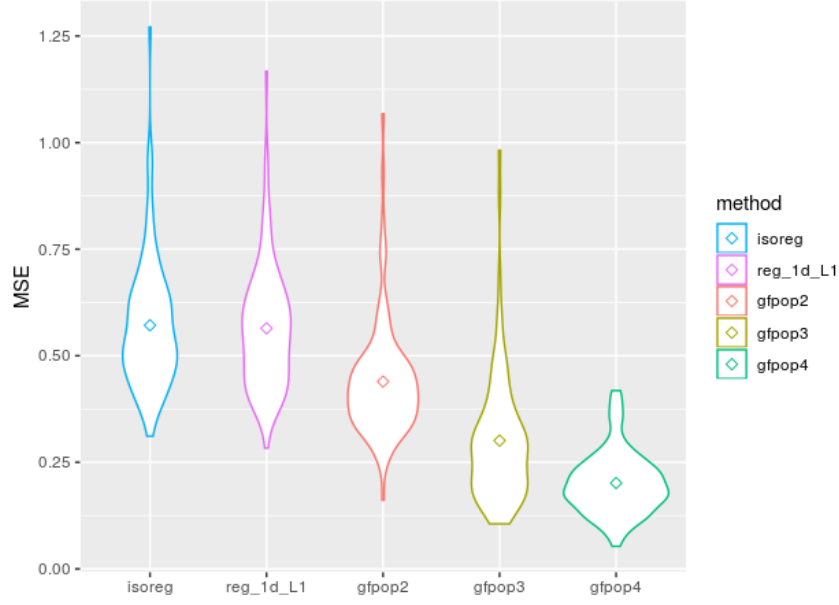


Figure 17: Violin plots of the MSE for iso-step simulations with Student noise. The shape of the distribution is very similar for the 5 best methods considered.

Iso-step simulations	isoreg ℓ_2	reg_1d ℓ_1	reg_1d ℓ_2	gfpop1 $\beta = 0$ ℓ_2	gfpop2 $\beta = 0$ $K = 3\sigma$	gfpop3 $\beta = \beta_0$ ℓ_2	gfpop4 $\beta = \beta_0$ $K = 3\sigma$
Gauss \hat{D} (SD)	66.8 (7.0)	66.7 (7.0)	59.0 (6.0)	69.1 (7.6)	66.7 (7.6)	10.0 (0)	10.0 (0)
Student \hat{D} (SD)	69.6 (7.2)	69.4 (7.2)	63.2 (6.8)	70.5 (7.9)	71.0 (8.2)	10.1 (0.24)	10.0 (0)
Corrupted \hat{D} (SD)	40.9 (5.2)	40.8 (5.2)	47.8 (5.9)	41.5 (5.6)	61.6 (7.6)	11.2 (0.95)	10.0 (0.14)

Table 3: Mean number of segments over 100 simulations with 10^4 data-points for different algorithms on step-wise simulations. We consider three types of noise : Gaussian, Student and corrupted.

References

Toby Dylan Hocking, Guillem Rigai, Paul Fearnhead, and Guillaume Bourque. A log-linear time algorithm for constrained changepoint detection. *arXiv preprint arXiv:1703.03352*, 2017.

Rebecca Killick, Paul Fearnhead, and Idris A Eckley. Optimal detection of changepoints with a linear computational cost. *Journal of the American Statistical Association*, 107(500):1590–1598, 2012.

Guillem Rigai. A pruned dynamic programming algorithm to recover the best segmentations

- with 1 to k_{\max} change-points. *Journal de la Société Française de Statistique*, 156(4):180–205, 2015.
- Robert Maidstone, Toby Hocking, Guillem Rigaill, and Paul Fearnhead. On optimal multiple changepoint algorithms for large data. *Statistics and computing*, 27(2):519–533, 2017.
- Toby Hocking, Guillem Rigaill, and Guillaume Bourque. Peakseg: constrained optimal segmentation and supervised penalty learning for peak detection in count data. In Francis Bach and David Blei, editors, *Proceedings of the 32nd International Conference on Machine Learning*, volume 37 of *Proceedings of Machine Learning Research*, pages 324–332, Lille, France, 07–09 Jul 2015a. PMLR. URL <http://proceedings.mlr.press/v37/hocking15.html>.
- Sean Jewell, Toby Dylan Hocking, Paul Fearnhead, and Daniela Witten. Fast nonconvex deconvolution of calcium imaging data. *arXiv preprint arXiv:1802.07380*, 2018.
- R Baranowski and P Fryzlewicz. wbs: Wild binary segmentation for multiple change-point detection, 2014. *R package version*, 1, 2014.
- Richard E Barlow, David J Bartholomew, James M Bremner, and H Daniel Brunk. Statistical inference under order restrictions: The theory and application of isotonic regression. Technical report, Wiley New York, 1972.
- Quentin F Stout. Unimodal regression via prefix isotonic regression. *Computational Statistics & Data Analysis*, 53(2):289–297, 2008.
- Michael J Best and Nilotpal Chakravarti. Active set algorithms for isotonic regression; a unifying framework. *Mathematical Programming*, 47(1-3):425–439, 1990.
- Paul Fearnhead and Guillem Rigaill. Changepoint detection in the presence of outliers. *Journal of the American Statistical Association*, pages 1–15, 2018.
- Francis Bach. Efficient algorithms for non-convex isotonic regression through submodular optimization. In *Advances in Neural Information Processing Systems*, pages 1–10, 2018.
- Toby Hocking, Guillem Rigaill, and Guillaume Bourque. Peakseg: constrained optimal segmentation and supervised penalty learning for peak detection in count data. In *International Conference on Machine Learning*, pages 324–332, 2015b.
- Ivan E Auger and Charles E Lawrence. Algorithms for the optimal identification of segment neighborhoods. *Bulletin of mathematical biology*, 51(1):39–54, 1989.
- Alexander Tristan Maximilian Fisch, Idris Arthur Eckley, and Paul Fearnhead. A linear time method for the detection of point and collective anomalies. *arXiv preprint arXiv:1806.01947*, 2018.
- Brad Jackson, Jeffrey D Scargle, David Barnes, Sundararajan Arabhi, Alina Alt, Peter Gioumoussis, Elyus Gwin, Paungkaew Sangtrakulcharoen, Linda Tan, and Tun Tao Tsai. An algorithm for optimal partitioning of data on an interval. *IEEE Signal Processing Letters*, 12(2):105–108, 2005.
- Holger Dette and Dominik Wied. Detecting relevant changes in time series models. *Journal of the Royal Statistical Society: Series B (Statistical Methodology)*, 78(2):371–394, 2016.
- Franck Picard, Stephane Robin, Marc Lavielle, Christian Vaisse, and Jean-Jacques Daudin. A statistical approach for array cgh data analysis. *BMC bioinformatics*, 6(1):27, 2005.

- Yi-Ching Yao and Siu-Tong Au. Least-squares estimation of a step function. *Sankhyā: The Indian Journal of Statistics, Series A*, pages 370–381, 1989.
- Nancy R Zhang and David O Siegmund. A modified bayes information criterion with applications to the analysis of comparative genomic hybridization data. *Biometrics*, 63(1):22–32, 2007.
- Émilie Lebarbier. Detecting multiple change-points in the mean of gaussian process by model selection. *Signal processing*, 85(4):717–736, 2005.
- Yannick Baraud, Christophe Giraud, Sylvie Huet, et al. Gaussian model selection with an unknown variance. *The Annals of Statistics*, 37(2):630–672, 2009.
- Kaylea Haynes, Idris A Eckley, and Paul Fearnhead. Efficient penalty search for multiple changepoint problems. *arXiv preprint arXiv:1412.3617*, 2014.
- Guillem Rigai, Toby Hocking, Jean-Philippe Vert, and Francis Bach. Learning sparse penalties for change-point detection using max margin interval regression. In *Proc. 30th ICML*, pages 172–180, 2013.
- Chao Gao, Fang Han, and Cun-Hui Zhang. On estimation of isotonic piecewise constant signals. *arXiv preprint arXiv:1705.06386*, 2017.
- Peter Hall, JW Kay, and DM Titterton. Asymptotically optimal difference-based estimation of variance in nonparametric regression. *Biometrika*, 77(3):521–528, 1990.
- Gudrun Schleiermacher, Isabelle Janoueix-Lerosey, Agns Ribeiro, Jerzy Klijanienko, Jérôme Couturier, Galle Pierron, Vronique Mosseri, Alexander Valent, Nathalie Auger, Dominique Plantaz, Hervé Rubie, Dominique Valteau-Couanet, Franck Bourdeaut, Valérie Combaret, Christophe Bergeron, Jean Michon, and Olivier Delattre. Accumulation of segmental alterations determines progression in neuroblastoma. *Journal of Clinical Oncology*, 28(19):3122–3130, 2010. doi: 10.1200/JCO.2009.26.7955. URL <https://doi.org/10.1200/JCO.2009.26.7955>. PMID: 20516441.
- Toby Dylan Hocking, Gudrun Schleiermacher, Isabelle Janoueix-Lerosey, Valentina Boeva, Julie Cappo, Oliver Delattre, Francis Bach, and Jean-Philippe Vert. Learning smoothing models of copy number profiles using breakpoint annotations. *BMC Bioinformatics*, 14(164), May 2013.
- T. D. Hocking and G. J. Rigai. SegAnnot: an R package for fast segmentation of annotated piecewise constant signals. HAL technical report 00759129, 2012.
- F. Afghah, A. Razi, and K. Najarian. A shapley value solution to game theoretic-based feature reduction in false alarm detection. *Neural Information Processing Systems (NIPS), Workshop on Machine Learning in Healthcare*, arXiv:1512.01680 [cs.CV], Dec. 2015.
- S. Mousavi and F. Afghah. Inter- and intra- patient ecg heartbeat classification for arrhythmia detection: A sequence to sequence deep learning approach. In *ICASSP 2019 - 2019 IEEE International Conference on Acoustics, Speech and Signal Processing (ICASSP)*, pages 1308–1312, May 2019. doi: 10.1109/ICASSP.2019.8683140.
- PhysioNet. *Reducing False Arrhythmia Alarms in the ICU*, 2015. URL <http://www.physionet.org/challenge/2015/>. accessed July 28, 2016.

- G. Clifford, I. Silva, B. Moody, Q. Li, D. Kella, A. Chahin, T. Kooistra, D. Perry, and R. Mark. False alarm reduction in critical care. *Physiological Measurement*, 37(8):5–23, 2016.
- J. Pan and W. J. Tompkins. A real-time qrs detection algorithm. *IEEE Transactions on Biomedical Engineering*, BME-32(3):230–236, March 1985. ISSN 0018-9294. doi: 10.1109/TBME.1985.325532.
- A. Agostinelli, I. Marcantoni, E. Moretti, A. Sbrollini, S. Fioretti, F. Di Nardo, and L. Burattini. Noninvasive fetal electrocardiography part i: Pan-tompkins’ algorithm adaptation to fetal r-peak identification. *The open biomedical engineering journal*, 11:1724, 2017.
- Patrick Mair, Kurt Hornik, and Jan de Leeuw. Isotone optimization in r: pool-adjacent-violators algorithm (pava) and active set methods. *Journal of statistical software*, 32(5): 1–24, 2009.
- C. Gao, F. Han, and C.-H. Zhang. On Estimation of Isotonic Piecewise Constant Signals. *arXiv e-prints*, May 2017.

A Some other graphs

Here are two graphs for models discussed in the main part of the paper.

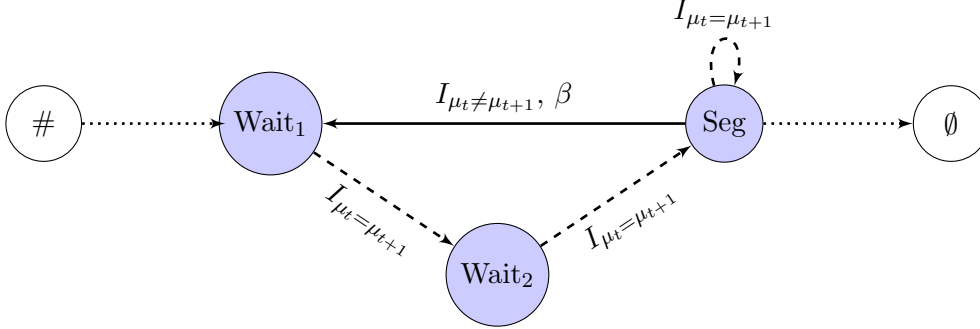


Figure 18: Graph for the at least 3 data-point per segment model. We have $\mathcal{S} = \{Wait_1, Wait_2, Seg\}$, the loss function is always the ℓ_2 . The penalty is omitted when equal to zero.

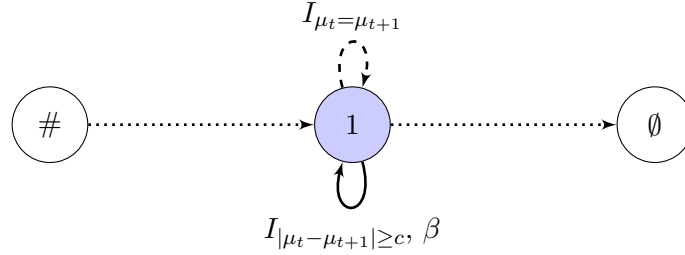


Figure 19: Graph for relevant change-point model. We have $\mathcal{S} = \{1\}$, the loss function is always the ℓ_2 . The penalty is omitted when equal to zero.

Below we provide a few other constraint models and their graphs.

- (Up - Down Relevant) It might make sense to consider sufficiently large changes. This is a simple modification of the Up - Down model (see Figure 6). The Dw to Up constraint $I_{\mu_t \leq \mu_{t+1}}$ can be replaced by $I_{c + \mu_t \leq \mu_{t+1}}$ for $c > 0$ or $I_{a\mu_t \leq \mu_{t+1}}$ for $a > 1$ if μ_t are positive. The graph is shown in Figure 20.
- (Up - Down with at least two datapoints) If one wants to detect peaks and is certain that segments are at least of length 2 it suffices to add two waiting states in the Up - Down graph. The graph of this model is given Figure 21.
- (Up - Isotonic Down) In the pulse detection example (Up - Exponentially Down model in Figure 7) if one is not sure of the exponential decrease it could make sense to consider an isotonic decrease. For this it suffices to consider two states $\mathcal{S} = \{Up, Dw\}$. Compared to the Up - Down model, described earlier, we add an additional transition from Dw to Dw with the constraint $I_{\mu_t \geq \mu_{t+1}}$. The graph of this model is given in Figure 22.
- (Isotonic Up - Isotonic Down) In the previous model one considers a sharp transition up. It might make sense to consider an isotonic increase. For this it suffices to add an edge from Up to Up in the previous model. Only transitions from Up to Dw and Dw to Up are penalised. The graph of this model is given in Figure 23.

- (Collective anomalies) Recently [Fisch et al. \[2018\]](#) proposed a collective anomaly and single outlier detection scheme. This model is encoded by two states $\mathcal{S} = \{\theta_0, Coll\}$. In the “normal” state the parameter is fixed to a user given θ_0 . In the collective anomaly state the parameter is in \mathbb{R} . There are four transitions. One from θ_0 to θ_0 with the biweight loss, and a constraint $I_{\mu_t = \mu_{t+1}}$. One from $Coll$ to θ_0 with the biweight loss, and a constraint $I_{\mu_t \neq \mu_{t+1}}$. One from $Coll$ to $Coll$ with the ℓ_2 loss, and a constraint $I_{\mu_t = \mu_{t+1}}$. One from θ_0 to $Coll$ with the ℓ_2 loss, a constraint $I_{\mu_t \neq \mu_{t+1}}$ and a penalty β . The graph of this model is given Figure 24.

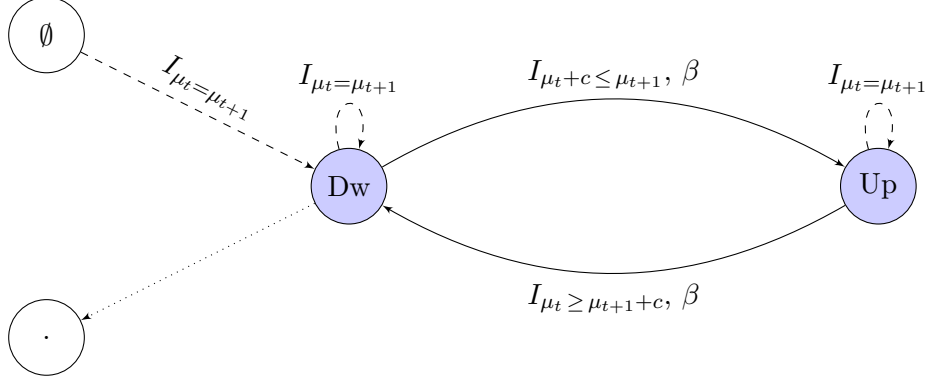


Figure 20: Graph for the Up-Down relevant model. We have $\mathcal{S} = \{Up, Dw\}$, the loss function is always the ℓ_2 . The penalty is omitted when equal to zero.

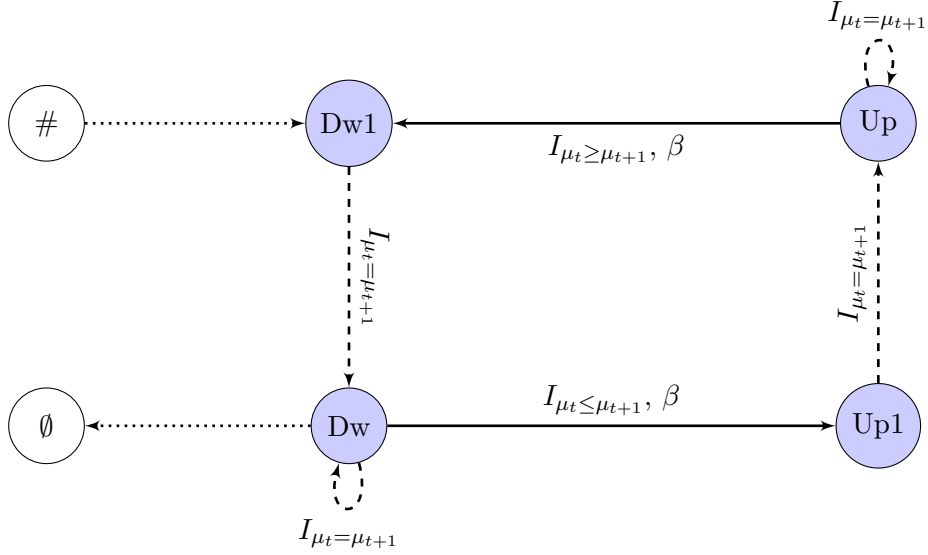


Figure 21: Graph for the Up-Down model with segments of size at least 2. We have $\mathcal{S} = \{Up1, Up, Dw1, Dw\}$. The loss function is always the ℓ_2 or the Poisson. The penalty is omitted when equal to zero.

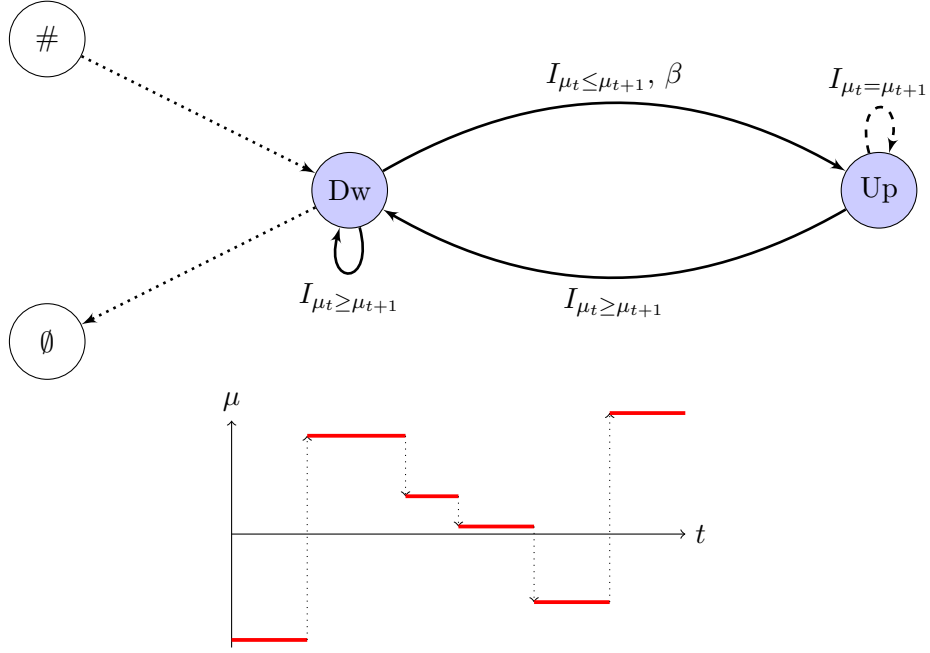


Figure 22: (Top) Graph for the up-down* change-point model. We have $\mathcal{S} = \{Dw, Up\}$, the loss function is always the ℓ_2 . The penalty is omitted when equal to zero. (Bottom) In red, a piecewise constant function validating the graph of constraints.

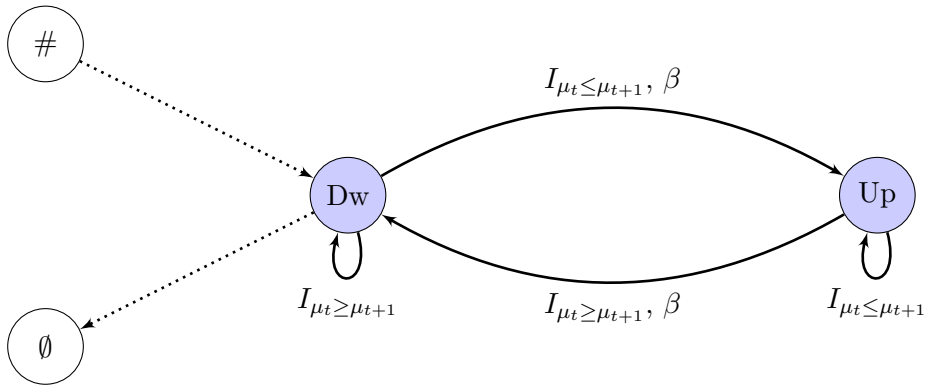


Figure 23: Graph for the up*-down* change-point model. We have $\mathcal{S} = \{Dw, Up\}$, the loss function is always the ℓ_2 . The penalty is omitted when equal to zero.

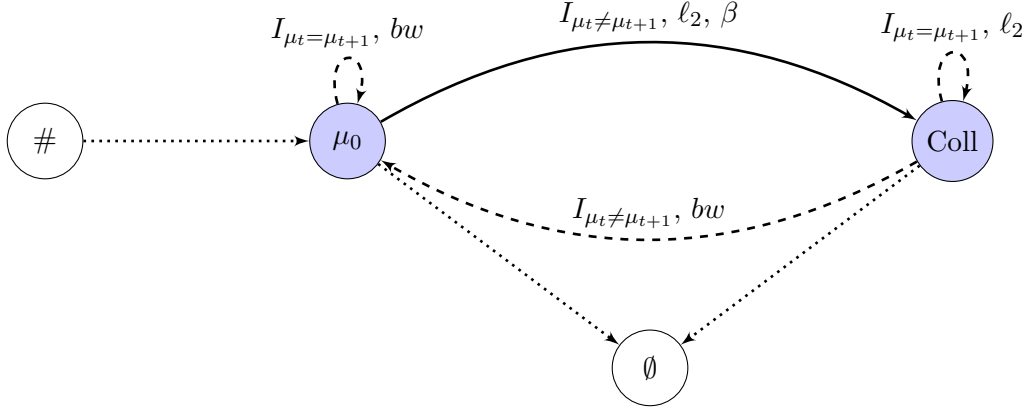


Figure 24: Graph for the model proposed in Fisch et al. [2018] We have $\mathcal{S} = \{\mu_0, Coll\}$. Note that the value of μ_0 is given and that the loss function is either the ℓ_2 or the biweight bw . The penalty is omitted when equal to zero.

B Update-rule proof

We recall here the update-rule (2) given at the end of Subsection 3.2.

$$Q_{n+1}^{s'}(\theta) = \min_{s|\exists \text{ edge}(s,s')} \left\{ O_n^{s,s'}(\theta) + \gamma_{(s,s')}(y_{n+1}, \theta) + \beta_{(s,s')} \right\}.$$

We name the path and vector realizing the best cost $Q_{n+1}^{s'}(\theta)$, defined in equation (1), p^* and μ^* . We call s^* the corresponding vector of states. We have $s_{n+1}^* = s'$, $\mu_{n+1}^* = \theta$ and

$$Q_{n+1}^{s'}(\theta) = \sum_{t=1}^{n+1} (\gamma_{e_t^*}(y_t, \mu_t^*) + \beta_{e_t^*}) = \sum_{t=1}^n (\gamma_{e_t^*}(y_t, \mu_t^*) + \beta_{e_t^*}) + (\gamma_{(s_n^*, s')}(y_{n+1}, \theta) + \beta_{(s_n^*, s')}).$$

We will first show that

$$\sum_{t=1}^n (\gamma_{e_t^*}(y_t, \mu_t^*) + \beta_{e_t^*}) = Q_n^{s_n^*}(\mu_n^*) = O_n^{s_n^*, s'}(\theta).$$

(Proof) Restricting the path p^* and the vector μ^* to their first n elements, by definition of $Q_n^{s_n^*}(\mu_n^*)$ we have $\sum_{t=1}^n (\gamma_{e_t^*}(y_t, \mu_t^*) + \beta_{e_t^*}) \geq Q_n^{s_n^*}(\mu_n^*)$. Also, given that a move from parameter μ_n^* to θ is a valid transition from state s_n^* to s' and by the definition of $O_n^{s_n^*, s'}(\theta)$, we have $Q_n^{s_n^*}(\mu_n^*) \geq O_n^{s_n^*, s'}(\theta)$.

We will now proceed by contradiction. Let us assume that $\sum_{t=1}^n (\gamma_{e_t^*}(y_t, \mu_t^*) + \beta_{e_t^*}) > O_n^{s_n^*, s'}(\theta)$. We name the path and vector realizing the $O_n^{s_n^*, s'}(\theta)$ p^+ and μ^+ . Extending this path and vector to $n+1$ with $s_{n+1}^+ = s'$ and $\mu_{n+1}^+ = \theta$ we get a better cost than p^* for $Q_{n+1}^{s'}(\theta)$ which is a contradiction.

So we have

$$Q_{n+1}^{s'}(\theta) = O_n^{s_n^*, s'}(\theta) + \gamma_{(s_n^*, s')}(y_{n+1}, \theta) + \beta_{(s_n^*, s')},$$

and considering all possible states at time n we get the update-rule.

C Backtracking

After running the Viterbi-like algorithm with update-rule (2), we need a backward procedure called backtracking to return the optimal change-point vector. First, we recover using Algorithm 1 the optimal vector of states $\hat{s} \in \{1, \dots, S\}^n$ and vector of means $\hat{\mu} \in \mathbb{R}^n$. We then find the best change-point vector $\hat{\tau} \subset \{1, \dots, n\}$ with Algorithm 2. The basic idea of Algorithm 1 is that if we knew \hat{s}_{t+1} and $\hat{\mu}_{t+1}$ we could recover first \hat{s}_t and then $\hat{\mu}_t$ taking the argmin of the update-rule (see lines 8 and 9 of Algorithm 1).

Algorithm 1 Backtracking \hat{s} and $\hat{\mu}$

```

1: procedure BACKTRACK( $(Q_1^1, \dots, Q_1^S), \dots, (Q_n^1, \dots, Q_n^S)$ )
2:  $\hat{\mu} \leftarrow$  empty vector of size  $n$ 
3:  $\hat{s} \leftarrow$  empty vector of size  $n$ 
4:  $(\hat{s}_n, \hat{\mu}_n) = \underset{s, \mu}{\operatorname{argmin}} \{Q_n^s(\mu)\}$ 
5:                                      $\triangleright$  We can impose a subset of arrival states  $\tilde{S} \subset \{1, \dots, S\}$ 
6:                                     by  $(\hat{s}_n, \hat{\mu}_n) \leftarrow \underset{\mu}{\operatorname{argmin}} \{Q_n^s(\mu)\}, s \in \tilde{S}$ 
7: for  $t = n - 1$  to  $t = 1$  do
8:    $\hat{s}_t = \underset{s | \exists \text{ edge}(s, \hat{s}_{t+1})}{\operatorname{argmin}} \left\{ O_t^{s, \hat{s}_{t+1}}(\hat{\mu}_{t+1}) + \gamma_{(s, \hat{s}_{t+1})}(y_{t+1}, \hat{\mu}_{t+1}) + \beta_{(s, \hat{s}_{t+1})} \right\}$ 
9:    $\hat{\mu}_t = \underset{\theta | I_{(\hat{s}_t, \hat{s}_{t+1})}(\mu, \hat{\mu}_{t+1})}{\operatorname{argmin}} \left\{ Q_t^{\hat{s}_t}(\mu) \right\}$ 
10: end for
11: return  $(\hat{s}, \hat{\mu})$ 

```

The obtained vectors \hat{s} and $\hat{\mu}$ are simplified removing repetitions of consecutive identical values: i.e. $\hat{s}_t = \sigma_0$ and $\hat{\mu}_t = m_0$ for $t = t_1, \dots, t_2$. In that case, the index t_2 is an element of the change-point vector. The vector of change-points can be built by a linear-in-time procedure described in Algorithm 2.

Algorithm 2 Change-point vector

```

1: procedure CHANGE-POINT( $\hat{s}, \hat{\mu}$ )
2:  $\hat{\tau} \leftarrow NULL$ 
3:  $t \leftarrow n$ 
4: while  $t \neq 0$  do
5:    $\hat{\tau} \leftarrow (t, \hat{\tau})$ 
6:   while  $(\hat{s}_t, \hat{\mu}_t) = (\hat{s}_{t-1}, \hat{\mu}_{t-1})$  do
7:      $t \leftarrow t - 1$ 
8:   end while
9: end while
10: return  $\hat{\tau}$ 

```

Notice that $\hat{\tau}$ is the `changepts` vector returned by the `gfpop` function. After removing repetitions in \hat{s} and $\hat{\mu}$, we also have \hat{s} equal to the `states` vector and $\hat{\mu}$ to the `parameters` vector.